Determination of bound-electronic and free-carrier nonlinearities in ZnSe, GaAs, CdTe, and ZnTe

A. A. Said, M. Sheik-Bahae, D. J. Hagan, T. H. Wei, J. Wang, J. Young,* and E. W. Van Stryland

Center for Research in Electro-Optics and Lasers, University of Central Florida, Orlando, Florida 32816

Received May 30, 1991; revised manuscript received August 30, 1991

We extend the application of the Z-scan experimental technique to determine free-carrier nonlinearities in the presence of bound electronic refraction and two-photon absorption. We employ this method, using picosecond pulses in CdTe, GaAs, and ZnTe at 1.06 μm and in ZnSe at 1.06 and 0.53 μm, to measure the refractive-index change induced by two-photon-excited free carriers (coefficient σ_r), the two-photon absorption coefficient β, and the bound electronic nonlinear refractive index n_2. The real and imaginary parts of the third-order susceptibility (i.e., n_2 and β, respectively) are determined by Z scans with low inputs, and the refraction from carriers generated by two-photon absorption (an effecitve fifth-order nonlinearity) is determined from Z scans with higher input energies. We compare our experimental results with theoretical models and deduce that the three measured parameters are well predicted by simple two-band models. n_2 changes from positive to negative as the photon energy approaches the band edge, in accordance with a recent theory of the dispersion of n_2 in solids based on Kramers–Kronig transformations [Phys. Rev. Lett. **65,** 96 (1990); IEEE J. Quantum Electron. **27,** 1296 (1991)]. We find that the values of σ_r are in agreement with simple band-filling models.

I. INTRODUCTION

The nonlinear-optical properties of semiconducting materials are being widely studied as potential components of various optical devices. Among the areas of interest are optical switching and optical limiting. Large nonlinearities in InSb,[1] GaAs,[2] and HgCdTe (Ref. 3) were observed and used in demonstrating all-optical switching at incident photon energies nearly resonant with the energy gap of the material. Large carrier nonlinearities are also observed in the transparency region where the carrier-excitation mechanism is two-photon absorption[4–8] (2PA). In the studies reported in Refs. 4–8 beam-distortion measurements at high irradiance were used to determine the nonlinear refraction, which was attributed solely to the free charge carriers, and the nonlinear refraction that was due to the bound electrons (electronic Kerr effect) was assumed to be negligible. However, picosecond time-resolved degenerate four-wave mixing experiments at much lower irradiance levels performed on ZnSe and CdTe in the presence of 2PA showed a large and fast third-order nonlinearity in addition to the higher-order carrier nonlinearity.[9] The 2PA-generated carrier refraction is an effective fifth-order process.[10]

In the study reported in Ref. 11, which used the sensitivity of the Z-scan method to monitor nonlinear refraction at low irradiance levels, a third-order nonlinearity was observed in ZnSe. This nonlinearity was attributed to n_2, the nonlinear refraction caused by bound electrons, as was explained theoretically in Ref. 12. At higher irradiance levels the refraction caused by the 2PA-generated free charge carriers becomes significant. In this paper we use the Z-scan technique[11,13] with picosecond pulses at several irradiance levels to determine the free-carrier refraction σ_r separately, in addition to the bound electronic n_2 and the 2PA coefficient β, in four different semiconductors: ZnSe at 1.06 and 0.532 μm and CdTe, GaAs, and ZnTe at 1.06 μm. With these measurements we are able to predict the contribution from each nonlinearity, given the experimental parameters (irradiance, pulse width, spot size, etc.). For example, we find here that the contribution of n_2 to the experiments of Refs. 4–7 was as large as 50% for the lowest inputs used in those measurements but rapidly decreased for higher inputs.

In Section 2 we briefly describe the Z-scan technique and the analysis for determining nonlinear absorption and refraction. Experimental results are given in Section 3. In Section 4 our measured values of the free-carrier refraction are compared with various theoretical models. We also compare our measured β and n_2 values with theoretical values. In Section 5 we describe a simple alternative method for estimating the different orders of nonlinear refraction, and we compare the results of this method with the results obtained by numerically fitting the experimental data.

2. Z SCAN

The Z-scan experimental arrangement is shown in Fig. 1. The transmittance of a focused Gaussian beam through an aperture in the far field is measured as a function of the sample position z with respect to the focal plane—hence the name Z scan. While the input energy is kept constant, the sample experiences a different incident field (amplitude and phase) at different z positions. Nonlinear refraction in the sample manifests itself as beam broadening or narrowing in the far field, thus changing the fraction of light passing through the aperture as the sample position is changed. Therefore the aperture transmittance is a function of the sample position z. As is explained in Ref. 13, the sign of the nonlinear refraction is readily obtained from a Z-scan signal. An increase in transmittance followed by a decrease in transmittance (peak–valley) denotes a negative nonlinear refraction, whereas a valley–peak configuration implies a positive nonlinearity. Removal of the aperture, i.e., collecting all

0740-3224/92/030405-10$05.00

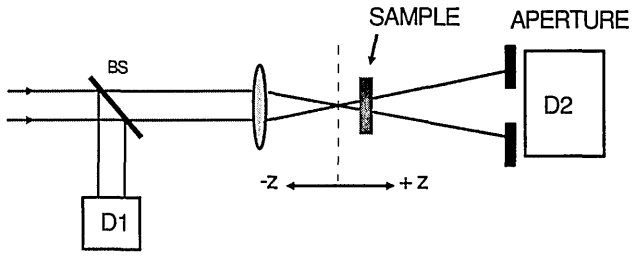

Fig. 1. Z-scan experimental setup. D_2/D_1 is measured as a function of the sample position z. D1, D2, detectors.

the transmitted light on detector D2, which we refer to as an open-aperture Z scan, will result in a flat response for a purely refractive nonlinearity. However, if nonlinear absorption is present, then the transmittance signal appears as an inverted Lorentzian, which has a minimum at $z = 0$ (the sample at the focal plane), where the irradiance is maximum. Nonlinear absorption suppresses the peak and enhances the valley in a closed-aperture Z scan (i.e., with the aperture in place), as is seen, for example, in Fig 3(b) below.

In order to analyze the Z-scan data we need to calculate the electric field at the aperture for any position z of the sample. This calculation can be performed by solving the nonlinear equations for propagation inside the sample and then those for propagation of the field in free space from the exit surface of the sample to the aperture. If the sample length is less than the confocal beam parameter, and if the phase changes in the field caused by the nonlinear interaction are not transformed into amplitude changes within the sample, then the sample is considered thin[14,15] (external self-action). Considering a thin sample and using the slowly varying envelope approximation, we can separate the wave equation into an equation for the phase and an equation for the irradiance[7]:

$$\frac{d\Delta\phi}{dz'} = k\Delta n, \tag{1}$$

$$\frac{dI}{dz'} = -(\alpha_0 + \beta I)I, \tag{2}$$

where Δn is the change in the index of refraction, k is the magnitude of the wave vector in free space, α_0 is the residual linear absorption, and z' is the propagation distance within the sample, which is to be distinguished from z, the sample position with respect to the focal plane.

In our experiments we used 30–40-ps pulses at irradiance levels below the critical value for free-carrier absorption.[16,17] Therefore Eq. (2) does not include free-carrier absorption. We verified that free-carrier absorption was negligible in our experiments by measuring the same 2PA coefficient at several irradiance levels. On the other hand, we find that the refraction arising from these free carriers cannot be neglected.[18] Thus Δn in Eq. (1) is written as

$$\Delta n = \gamma I + \sigma_r N, \tag{3}$$

where γ is the nonlinear index that is due to the bound electrons and is related to the usual nonlinear index n_2 through $n_2(\text{esu}) = (cn_0/40\pi)\gamma(\text{m}^2/\text{W})$, with c the speed of light in meters per second and σ_r the change in the index of refraction per unit photoexcited charge-carrier density N. If 2PA is the only mechanism for generating carriers, the carrier-generation rate is given by

$$\frac{dN}{dt} = \frac{\beta I^2}{2\hbar\omega}. \tag{4}$$

Here we neglect the loss of carriers through recombination and diffusion because these processes occur on time scales longer than the picosecond pulses that we use in the experiments. Thus the carrier nonlinearity [$\sigma_r N$ in Eq. (3)] is proportional to a temporal integral of I^2, resulting in an effective fifth-order nonlinearity; this conclusion is reached by the same reasoning that makes the index change caused by single-photon-absorption-generated free carriers an effective third-order effect.[19] In the 2PA case this fifth-order nonlinearity is a sequential $\text{Im}[\chi^{(3)}]$ process (i.e., 2PA) followed by a $\text{Re}[\chi^{(1)}]$ process (i.e., a linear index change from the carriers). The existence of two nonlinearities of different orders and different decay times was also observed by Canto-Said *et al.*[9] for picosecond degenerate four-wave mixing. The fast nonlinearity has a third-order dependence on the incident irradiance [$\chi^{(3)}$ effect], whereas the carrier nonlinearity has a fifth-order dependence. The degenerate four-wave mixing technique cannot identify the nature (refractive or absorptive) or the sign of these nonlinearities. Also, from examination of the two terms on the right-hand side of Eq. (3), it is clear that the electronic Kerr effect (γI) will be dominant at low irradiance levels, whereas the free-carrier refraction ($\sigma_r N$) will dominate at high irradiance levels.

The irradiance at the exit surface of the sample is obtained from Eq. (2) as

$$I(L, r, t, z) = \frac{I(0, r, t, z)\exp(-\alpha_0 L)}{1 + q(r, t, z)}, \tag{5}$$

where $q(r, t, z) = \beta I(0, r, t, z)L_{eff}$, $L_{\text{eff}} = [1 - \exp(-\alpha_0 L)]/\alpha_0$, and z is again the sample position. Here the irradiance within the sample is quoted after Fresnel reflections are taken into account. This irradiance is taken as a Gaussian in space and time, given by

$$I(0, r, t, z) = \frac{I_0 \exp[-2(r/w_0)^2 - (t/t_0)^2]}{1 + (z/z_0)^2}, \tag{6}$$

with $z_0 = \pi w_0^2/\lambda$. Removing the aperture in Fig. 1 is analogous to placing detector D2 at the exit surface of the sample. Such an open-aperture Z scan allows us to ignore the phase changes, and Eq. (5) leads to the normalized transmittance as calculated in Ref. 11 after integration over the spatially and temporally Gaussian pulse:

$$T(z) = \frac{1}{\pi^{1/2} q(0, 0, z)} \int_{-\infty}^{\infty} \ln[1 + q(0, 0, z)\exp(-\tau^2)]d\tau. \tag{7}$$

The only unknown parameter in Eq. (7) is β in $q(0, 0, z)$, which implies that an open-aperture Z scan will give the 2PA coefficient. Figure 2 shows a plot of $T(0)$ as a function of $q(0, 0, 0) = \beta I_0 L_{\text{eff}}$. This curve can be used in an open-aperture Z-scan transmittance measurement to determine β directly. At still higher irradiance levels free-carrier absorption must be included in Eq. (2), and an open-aperture Z scan could also be used to determine the free-carrier absorption. With β known from low-irradiance open-aperture Z-scan data, high-irradiance data will permit calculation of the free-carrier absorption

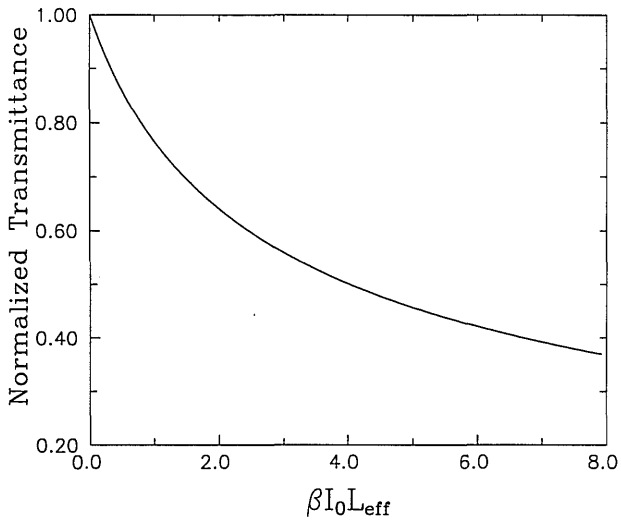

Fig. 2. Normalized transmittance for an open-aperture Z scan at $z = 0$ as a function of $\beta I_0 L_{\text{eff}} = q(0,0,0)$. From this curve β can be determined without fitting the data.

cross section. However, as is mentioned above, all the experiments reported here are below the critical irradiance for free-carrier absorption.

The total phase change $\Delta\phi$ experienced by the beam is obtained by integrating Eq. (1), using Eq. (3), to give[7]

$$\Delta\phi(r,t,z) = \frac{k\gamma}{\beta}\ln[1 + q(r,t,z)] + \frac{k\sigma_r}{2\hbar\omega\beta}\int_{-\infty}^{t} dt' F(t'), \quad (8)$$

where

$$F(t) = \alpha_0 \ln[1 + q(r,t,z)] - \frac{q(r,t,z)}{L_{\text{eff}}}\left[1 - \frac{\exp(-\alpha_0 L)}{1 + q(r,t,z)}\right]. \quad (9)$$

The field at the exit surface of the sample is completely determined by Eqs. (5) and (8) [i.e., $E \propto I^{1/2}\exp(i\Delta\phi)$], where the reflection losses are included. The field at the aperture is determined by the Huygens–Fresnel propagation integral[20]:

$$E_a(r,t,z) = \frac{2\pi}{i\lambda(d-z)}\exp\left[\frac{i\pi r^2}{\lambda(d-z)}\right] \times \int_0^{\infty} r' dr' E(L,r',t,z)\exp\left[\frac{i\pi r'^2}{\lambda(d-z)}\right] \times J_0\left[\frac{2\pi r r'}{\lambda(d-z)}\right], \quad (10)$$

where d is the distance between the aperture and the focal plane. The transmitted power through the aperture is given by

$$P_T(z,t) = c\epsilon_0 n_0 \pi \int_0^{r_a} |E_a(r,t)|^2 r dr, \quad (11)$$

and the normalized transmittance is

$$T(z,S) = \frac{\int_{-\infty}^{\infty} P_T(t)dt}{S\int_{-\infty}^{\infty} P_i(t)dt}, \quad (12)$$

where $P_i(t) = I(r = 0, t, z = 0)(\pi w_0^2/2)$ is the input power. Here S is the linear aperture transmittance given by $S = 1 - \exp(-2r_a^2/w_a^2)$, with r_a and w_a being the aperture radius and the beam radius at the aperture in the linear regime, respectively. Equation (7) is identical to Eq. (12) for $S = 1$. Note that Eq. (12) includes the losses, if any, by 2PA as well as losses that are due to the aperture. In what follows we compare the numerical evaluation of Eqs. (7) (nonlinear absorption only) and Eq. (12) with the experimental results.

3. EXPERIMENTAL RESULTS

We performed Z-scan experiments on three II–VI semiconductors, ZnSe, CdTe, and ZnTe, and a III–V semiconductor, GaAs. ZnSe is a two-photon absorber at 532 nm, whereas the other three samples are two-photon absorbers at 1.06 μm. We first discuss experiments with ZnSe at 532 nm. In the following measurements the irradiance values were carefully determined. The pulse width was measured by performing autocorrelation experiments and was monitored for each laser firing as described in Ref. 7, and the beam radius was determined from several pinhole beam scans. Using the Z-scan property $\Delta Z_{p-v} \simeq 1.7 z_0$, we double-checked the beam scan results by performing Z-scan experiments on CS_2 (see Ref. 11). The energy values were measured by calibrating the reference detector against a calibrated Gentec energy meter.

A. 0.532-μm Results

With 27-ps (FWHM) pulses at 532 nm from a frequency-doubled Nd:YAG laser we performed Z scans at different input energies on a 2.7-mm-thick polycrystalline sample of ZnSe grown by chemical-vapor deposition. The sample has an energy gap of 2.67 eV.[21] The beam was focused to a radius of $w_0 \simeq 25$ μm. First an open-aperture Z scan was performed at $I_0 = 0.21$ GW/cm^2. All the experimental irradiances reported here are those within the sample (i.e., Fresnel reflections are taken into account). In Fig. 3(a) we plot the experimental data and the theoretical fit obtained by setting $\beta = 5.8 \pm 1.2$ cm/GW in Eq. (7). This is within 5% of the value of 5.5 cm/GW reported in Ref. 7. The fitting uncertainties for this measurement and for the measurements listed below were ±10%, but the overall experimental uncertainty is ±20%, arising mainly from uncertainties in the irradiance calibration. With the 40% aperture ($S = 0.4$) another Z scan was performed at the same irradiance. In this case the measurement is sensitive to both nonlinear refraction and nonlinear absorption. Experiments on ZnSe were conducted at irradiance levels from 0.21 to 2.4 GW/cm^2. At the lowest irradiance we expect the change in the index of refraction to be due mostly to the third-order anharmonic motion of the bound electrons.[11] With $\beta = 5.8$ cm/GW and neglecting free-carrier refraction (i.e., $\sigma_r = 0$), we fitted the experimental data of Fig. 3(b), using $\gamma = -6.8 \times 10^{-14}$ cm^2/W ($n_2 = -4.4 \times 10^{-11}$ esu) in Eq. (12). The negative sign of n_2 can easily be deduced from the peak–valley feature of the Z-scan signal. Note that the minus was inadvertently omitted in Ref. 11. The same experiment was repeated at $I_0 = 2.4$ GW/cm^2. The free-carrier contribution to the refraction becomes significant at this irradiance level. In all, 10 Z scans were performed (5 open aperture and 5 closed). Using an iterative approach to best-fit all the data, we found a better fit by modifying n_2 from $-4.4 \times$

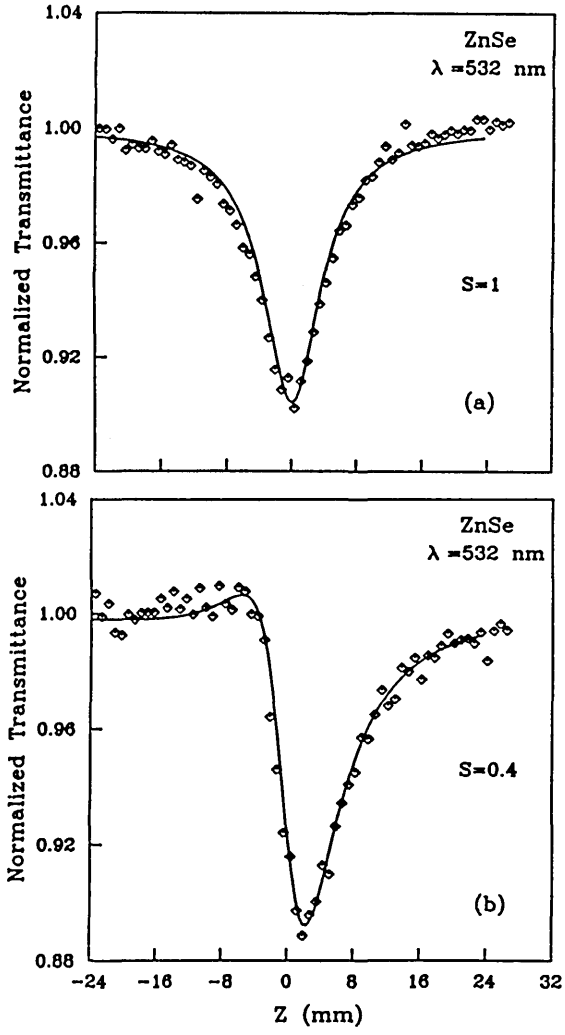

Fig. 3. Normalized Z-scan data of a 2.7-mm ZnSe sample measured with 27-ps (FWHM) pulses and $\lambda = 532$ nm at low irradiance ($I_0 = 0.21$ GW/cm^2). The solid curves are the theoretical fits. (a) Open-aperture data ($S = 1$) were fitted with $\beta = 5.8$ cm/GW. (b) 40%-aperture data were fitted with $\beta = 5.8$ cm/GW and $n_2 = -4.4 \times 10^{-11}$ esu.

10^{-11} to $-(4.0 \pm 0.8) \times 10^{-11}$ esu and using $\sigma_r = -(0.8 \pm 0.2) \times 10^{-21}$ cm^3. Thus there is a small contribution from σ_r, even at the lowest irradiance level. The data and fit for $I_0 = 0.57$ and $I_0 = 2.4$ GW/cm^2 are shown in Figs. 4(a) and 4(b), respectively. The agreement between experiment and theory is remarkable, given that the change in transmittance between the peak and the valley ranges from approximately 10% in Fig. 3(b) to 90% in Fig. 4(b). The absolute errors in the measurement of σ_r of $\pm 25\%$ are only slightly larger than those for β and γ, even though the nonlinearity is of a higher order. This result occurs in part because the calculation of σ_r depends on the products βI_0 and γI_0, which we know more accurately than β or γ separately.

B. 1.06-μm Results

All the Z-scan experiments discussed below were performed with 40-ps pulses (FWHM) from a Nd:YAG laser focused to $w_0 \simeq 40$ μm. CdTe has an energy band gap of 1.44 eV, which makes it a two-photon absorber at 1.06 μm. The sample used is undoped, polycrystalline, and 3 mm thick.[21] Following the same procedure as for ZnSe, we were able to determine $\beta = 26 \pm 5$ cm/GW, as compared with 22 and 15 cm/GW for two different samples reported in Ref. 7. We also found $\gamma = -(3.0 \pm 0.6) \times 10^{-13}$ esu or $n_2 = -(2.0 \pm 0.4) \times 10^{-10}$ esu and $\sigma_r = -(5.0 \pm 1.2) \times 10^{-21}$ cm^3. The theoretical fit with Eq. (12) used for one of the eight Z-scan experiments performed on CdTe with the above values is shown in Fig. 5; the closed-aperture data were taken at $I_0 = 0.3$ GW/cm^2.

2PA and nonlinear refraction in GaAs were used for optical limiting in Ref. 18. However, the bound electronic and free-carrier refractive nonlinearities were not measured separately. Recently high-irradiance measurements were used to estimate σ_r in GaAs while refractive contributions from n_2 were ignored.[22] We followed the same steps taken in determining the nonlinearities for ZnSe and CdTe, using data from eight Z scans. Figure 6 shows the theoretical fit to the experimental data extracted from a closed-aperture Z-scan experiment at $I_0 = 0.45$ GW/cm^2 on a 1.2-mm-thick undoped single crys-

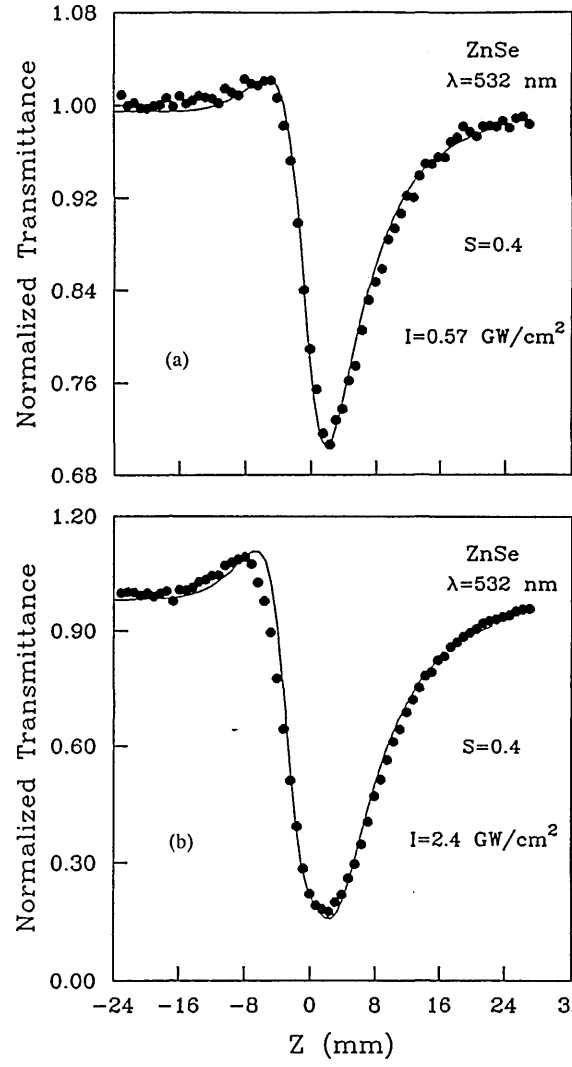

Fig. 4. Closed-aperture Z-scan data ($S = 0.4$) and theoretical fits (solid curves) of the ZnSe sample taken at high irradiance levels of (a) $I_0 = 0.57$ GW/cm^2 and (b) $I_0 = 2.4$ GW/cm^2, where free-carrier refraction is significant. The data in (a) and (b) were fitted with $\beta = 5.8$ cm/GW, $n_2 = -4.0 \times 10^{-11}$ esu, and $\sigma_r = -0.8 \times 10^{-21}$ cm^3.

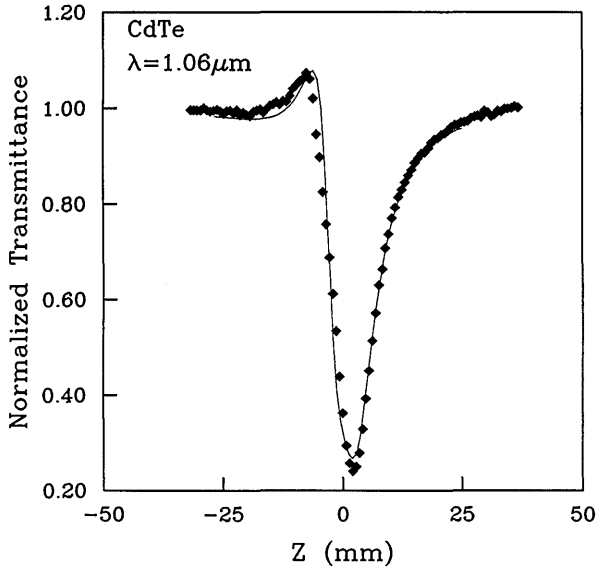

Fig. 5. Closed-aperture Z-scan data ($S = 0.4$) for a 3-mm CdTe sample with 1.06-μm, 40-ps (FWHM) pulses at $I_0 = 300$ MW/cm^2. The theoretical fit (solid curve) was obtained with $\beta = 26$ cm/GW, $n_2 = -2.0 \times 10^{-10}$ esu, and $\sigma_r = -5.0 \times 10^{-21}$ cm^3.

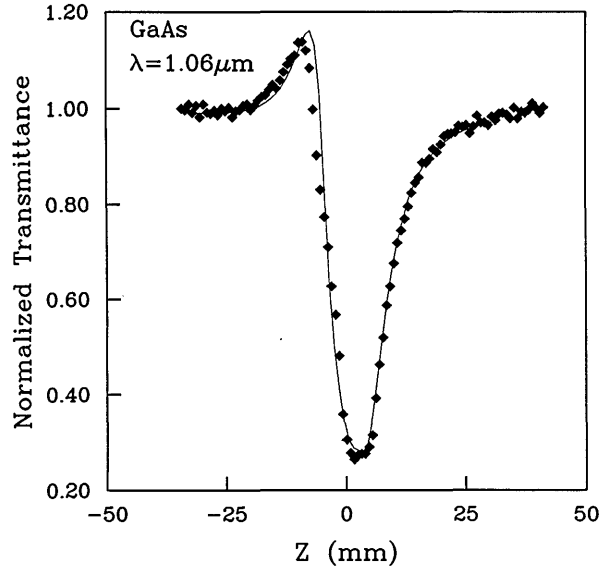

Fig. 6. Closed-aperture Z-scan data ($S = 0.4$) for a 1.2-mm GaAs sample with 1.06-μm, 40-ps (FWHM) pulses at $I_0 = 450$ MW/cm^2. The theoretical fit (solid curve) was obtained with $\beta = 26$ cm/GW, $n_2 = -2.7 \times 10^{-10}$ esu, and $\sigma_r = -6.5 \times 10^{-21}$ cm^3.

tal of GaAs of orientation (110) perpendicular to the surface.[21] We saw no greater than a 10% anisotropy on changing polarization in any of the nonlinear coefficients. We measured $\beta = 26 \pm 5$ cm/GW (23 cm/GW in Ref. 7 and 26 cm/GW in Ref. 15), $n_2 = -(2.7 \pm 0.5) \times 10^{-10}$ esu and $\sigma_r = -(6.5 \pm 1.6) \times 10^{-21}$ cm^3.

Z scans at 1.06 μm were performed on a 2-mm-thick single crystal of ZnTe oriented with the (111) plane perpendicular to the propagation direction.[22] The shape of the Z-scan signal is drastically different from those of the other semiconductor materials. For example, a peak–valley or valley–peak signature is not obvious from the data of Fig. 7. In the three materials mentioned above, the bound electronic nonlinearity was found to be negative. Thus the bound- and free-carrier refraction are of the same sign, and so they add. This explains why the Z-scan signal maintains its peak–valley feature at low [Fig. 3(b)] and high (Fig. 4) irradiance levels. For each of these semiconductors the incident photon energy was below but close to the band edge (i.e., well above the 2PA edge). The band gap of ZnTe, 2.26 eV, is almost resonant with the two-photon transition, 2.34 eV.

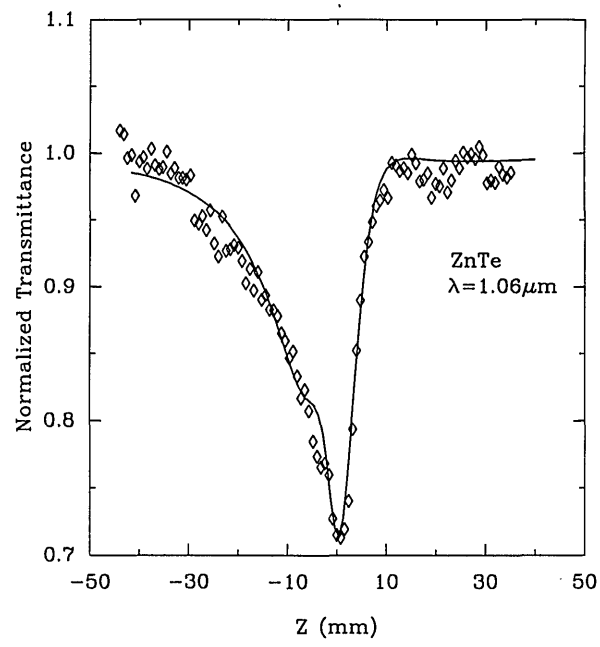

Fig. 7. Closed-aperture Z-scan data ($S = 0.4$) and theoretical fit (solid curve) of the ZnTe sample at $I_0 = 1.4$ GW/cm^2. The data were fitted with $\beta = 4.2$ cm/GW, $n_2 = +8.3 \times 10^{-11}$ esu, and $\sigma_r = 0.75 \times 10^{-21}$ cm^3. No definite peak–valley or valley–peak signature can be observed.

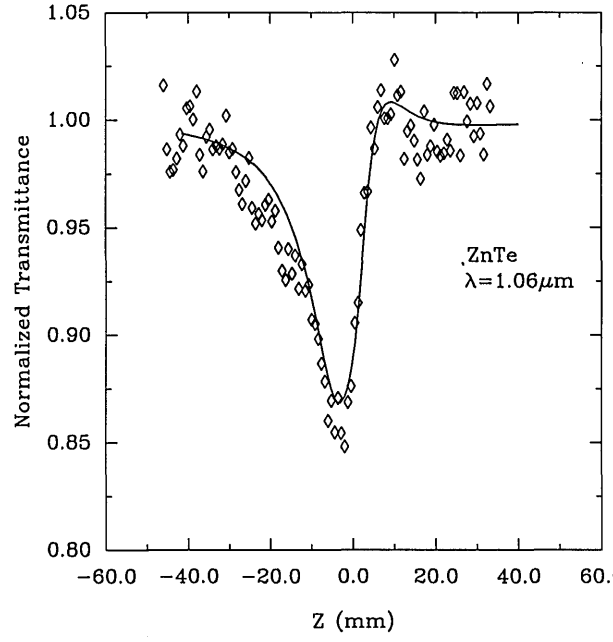

Fig. 8. Closed-aperture Z-scan data ($S = 0.4$) and theoretical fit (solid curve) of the ZnTe sample at $I_0 = 0.6$ GW/cm^2. The data were fitted with the same parameters used in Fig. 7. The valley–peak configuration indicates that the positive bound electronic Kerr effect is dominant at this irradiance level.

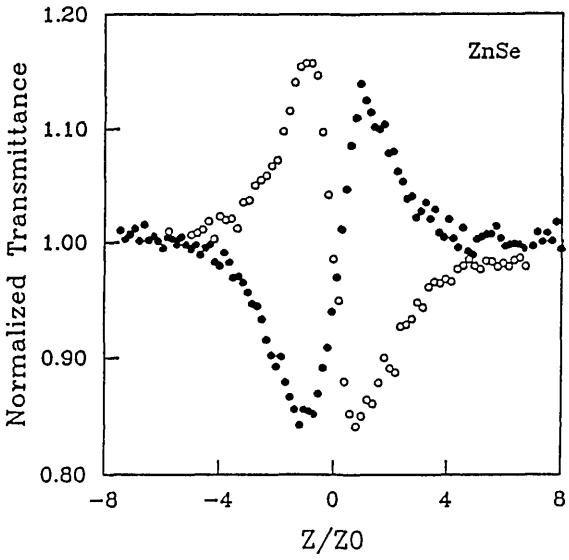

Fig. 9. Closed-aperture ($S = 0.4$) Z-scan experimental data of ZnSe at 1.06 μm (filled circles) and 532 nm (open circles) in units of $z_0 = \pi w_0^2/\lambda$. This figure clearly shows the dispersion in n_2 as it changes its sign from positive at 1.06 μm to negative at 532 nm.

Using the relatively low irradiance of $I_0 = 0.6$ GW/cm^2, for which n_2 is expected to dominate, we observed a valley–peak signal, indicating a positive n_2, as is shown in Fig. 8. The positive sign of n_2 is consistent with theoretical expectations, as is discussed in Section 4. At the input irradiance of $I_0 = 1.4$ GW/cm^2 used for the data of Fig. 7, the negative free-carrier refraction becomes significant but not dominant. At this irradiance the two effects with different signs compete to give the unusual shape of the Z-scan data. We were unable to go to higher irradiance levels because of the low damage threshold of the sample. As in the other semiconductors, the 2PA coefficient was obtained from open-aperture Z-scan data. The measured value is $\beta = 4.2 \pm 1.1$ cm/GW (4.5 cm/GW in Ref. 7). The data in Figs. 7 and 8 were fitted with $\gamma = +(1.2 \pm 0.4) \times 10^{-13}$ cm^2/W ($n_2 = +(8.3 \pm 2.5) \times 10^{-11}$ esu) and $\sigma_r = -(0.75 \pm 0.25) \times 10^{-21}$ cm^3. The errors in these values are somewhat higher than for the other materials because data from only four Z scans could be used.

We also measured n_2 in ZnSe at 1.06 μm, where two-photon absorption is not present. We obtained $n_2 = +(1.7 \pm 0.3) \times 10^{-11}$ esu. In Fig. 9 we plot closed-aperture ($S = 0.4$) Z scans obtained in ZnSe at 1.06 and 0.53 μm, showing the change in sign of n_2. For Fig. 9 the nonlinear absorption was removed from the 0.53-μm data by division. In Ref. 11 we showed that dividing the closed-aperture Z-scan data by the open-aperture data approximates the purely refractive Z scan (also see Section 5). This observed dispersion in n_2 is consistent with the recent theory of Refs. 12 and 23 and is discussed further in Section 4.

4. COMPARISONS BETWEEN EXPERIMENT AND THEORY

In this section we compare our experimental results with those of proposed theoretical models for the different nonlinearities involved. First, our measured values of the 2PA coefficients agree well with earlier reported values.[7,18] Van Stryland *et al.*[7] give a detailed comparison of their experimental results with existing theoretical models[24,25] for 2PA; their results showed remarkably good agreement with simple two-parabolic-band second-order perturbation theory. Listed in Table 1 are our experimental values of β compared with experimental and theoretical values from Ref. 7. Also consistent with the results of Ref. 7, the only significant deviation between experiment and theory was for ZnTe, in which β is approximately four times larger than predicted by this simple model. However, in ZnTe two photons couple states only 3% above the gap, where exciton enhancement and impurity effects may be expected to be important.[26]

The n_2 values of our results are compared in Table 1 with those calculated from the theoretical model of Sheik-Bahae *et al.*[12,23] This theory relates n_2 to the nonlinear absorption by using a nonlinear Kramers–Kronig transformation in a relation similar to that between the linear absorption and index of refraction. The nonlinear absorption was calculated by using two parabolic bands and includes contributions from 2PA as well as from electronic Raman and ac-Stark effects. References 12 and 23 also show that n_2 is inversely proportional to the fourth power of the energy gap. The trend in n_2 as a function of the ratio of photon energy to band-gap energy[23] shows small positive values for small ratios; this function slowly rises to a broad resonance peak at the 2PA edge and then decreases, eventually becoming negative between the two-photon and single-photon absorption edges. Thus the change from negative values of n_2 for semiconductors in which two photons couple states well above the gap (i.e., ZnSe, GaAs, and CdTe) to a positive value for ZnTe, in which two photons couple states only 3% above the gap, is expected. Also expected is the positive value of n_2 in ZnSe at 1.06 μm, where 2PA is not energetically allowed. The excellent agreement between the predicted and mea-

Table 1. Comparison of Experimental and Theoretical Values of n_2 and Two-Photon Absorption Coefficient β

Material	λ (nm)	n_0	n_2 (10^{-11} esu)		β (cm/GW)		
			Exp.[a]	Theor.[b]	Exp.[a]	Exp.[c]	Theor.[c]
ZnSe	532	2.70	−4.0	−3.8	5.8	5.5	4.27
CdTe	1064	2.84	−20	−21	26	22	25.1
GaAs	1064	3.43	−27	−31	26	23	19.7
ZnTe	1064	2.79	83	54	4.2	4.5	0.89

[a] This study.
[b] Ref. 23.
[c] Ref. 7.

Table 2. Contributions to the Change in the Index of Refraction Caused by Plasma and Blocking from Various Interband Transitions[a]

	Plasma Electron	Blocking Electron hh-c	Blocking Electron lh-c	Plasma h-Hole	Blocking h-Hole hh-c	Plasma l-Hole	Blocking l-Hole lh-c
ZnSe	20%	33%	23%	4%	16%	2%	2%
CdTe	27%	23%	21%	7%	15%	4%	3%
GaAs	34%	25%	24%	3%	10%	2%	2%

[a] Here c, hh, and lh refer to the conduction, heavy-hole, and light-hole bands, respectively.

sured n_2 values, including the sign change, is seen from Table 1.

We compare our results for the nonlinear refraction caused by free carriers to two different band-filling models (BF's). These models are the model attributed to Aronov *et al.*[27] and Auston *et al.*[28] (BF1) and the dynamic Moss–Burstein model with Boltzmann statistics[19,29,30] (BF2). In these theories the change in refraction that is due to carriers is independent of the means of carrier generation. In BF1 the nonlinear refraction that is due to free carriers is calculated directly from the real part of the complex dielectric function. The creation of N free electrons in the conduction band is accompanied by the elimination of N bound electrons in the valence band. For off-resonance excitation ($\hbar\omega < E_g$) the change in the index of refraction is given by[28]

$$\Delta n = -\frac{2\pi N e^2}{n_0 \omega^2 m_{cv}} \frac{E_g^2}{E_g^2 - (\hbar\omega)^2}, \tag{13}$$

where m_{cv} is the reduced effective mass of the electrons in the conduction band and the holes in the valence band. In Eq. (13) the hot-carrier effects were neglected because the carriers reach the band edge (thermal equilibrium with the lattice) within 2 ps,[28] which is short compared with our 27- and 40-ps pulses.

In BF2 the free carriers block the absorption at frequencies higher than the energy gap by filling the available states in the conduction and the valence bands. This model uses a Kramers–Kronig integral on this change in absorption. The total change in the index of refraction, including contributions from electrons, heavy holes, and light holes, is given by Wherrett *et al.* as [29]

$$\Delta n = -\frac{2\pi e^2}{n_0 \omega^2}\left\{\frac{\Delta N_c}{m_c}\left[1 + Z\left(\frac{m_{ch}}{m} J_{hc} + \frac{m_{cl}}{m} J_{lc}\right)\right] + \frac{\Delta P_h}{m_h}\left(1 + Z\frac{m_{ch}}{m} J_{hh}\right) + \frac{\Delta P_l}{m_l}\left(1 + Z\frac{m_{cl}}{m} J_{ll}\right)\right\}, \tag{14}$$

where

$$Z = \frac{4}{3\pi^{1/2}} \frac{mP^2}{\hbar^2 k_B T}, \tag{15}$$

$$J_{ij} = \int_0^\infty \frac{x^2 \exp(-x^2)}{x^2 + a_{ij}} dx, \tag{16}$$

$$a_{ij} = \frac{E_g - \hbar\omega}{k_B T} \frac{m_{ci}}{m_j}. \tag{17}$$

m is the electron mass, e is the electron charge, k_B is the Boltzmann constant, T is the temperature in kelvins, P is the Kane momentum[31] given by $E_p = 2P^2 m/\hbar^2$, and E_p is approximately 21 eV for semiconductors. ΔN and ΔP represent the photogenerated electron and hole densities, and the subscripts c, h, and l represent the conduction, heavy-hole, and light-hole bands, respectively. i and j are dummy subscripts that represent c, h, or l. ΔP_h and ΔP_l are given by[29]

$$\frac{\Delta N_c}{\Delta P_h} \simeq 1 + \left(\frac{m_l}{m_h}\right)^{3/2}, \qquad \frac{\Delta N_c}{\Delta P_l} \simeq 1 + \left(\frac{m_h}{m_l}\right)^{3/2}. \tag{18}$$

Equation (14) is an approximation that is adequate for near-resonance radiation. Off resonance, as in 2PA, we find that J_{ij} should be replaced by F_{ij}, where F is defined as

$$F_{ij} = -2J\left(\frac{m_{ci}}{m_j}\frac{E_g}{k_B T}\right) + J\left(\frac{m_{ci}}{m_j}\frac{E_g - \hbar\omega}{k_B T}\right) + J\left(\frac{m_{ci}}{m_j}\frac{E_g + \hbar\omega}{k_B T}\right). \tag{19}$$

For $\hbar\omega \simeq E_g$ and $E_g \gg k_B T$, the first and third terms on the right-hand side of Eq. (19) are extremely small compared with the second term; thus it is reasonable to neglect them, as was done in Eq. (14).[19,29] In 2PA experiments $E_g - \hbar\omega$ is comparable with E_g, and all three terms in Eq. (19) need to be retained.

The electrons' contribution to the index change is ΔN_c of Eq. (14), and this term includes blocking caused by electron transitions from the heavy-hole band and the light-hole band in addition to the change in the electron population in the conduction band. ΔP_h and ΔP_l give the contributions of the holes. Table 2 lists the contribution of each of these effects for ZnSe, CdTe, and GaAs. In the calculations for Table 2 F_{ij} was used rather than J_{ij}. It is seen from Table 2 that the change in the index of refraction from transitions between the light-hole band and the conduction band (electron blocking, light-hole blocking, and free-light-hole generation) contributes ≈27% for all three semiconductors listed. Thus it is reasonable to use the approximation of a two-band model when only transitions from the heavy-hole band to the conduction band are considered. In our experiments the low-temperature condition, or $|\hbar\omega - E_g| \gg k_B T$, is still satisfied; for example, in the worst case, that of GaAs, $|\hbar\omega - E_g| = 0.25$ eV, and at room temperature $k_B T \simeq 0.025$ eV. Examining J_{ij} in Eq. (16), we see for $a_{ij} \gg 1$ that $J_{ij} \simeq \pi^{1/2}/4a$. Substituting this value for J_{ij} into Eq. (19), we find that F_{ij} is proportional to $x^2/(1 - x^2)$, where $x = \hbar\omega/E_g$. Assuming a two-band model and substituting F_{ij} for J_{ij} in Eq. (14) shows that the change in the index of refraction that is due to the carrier transition blocking is

$$\Delta n(\text{blocking}) \propto (\hbar\omega)^2/[E_g^2 - (\hbar\omega)^2], \tag{20}$$

Table 3. Comparison of Experimental and Theoretical Values for the Index Change per Unit Carrier Density σ_r [a]

Material	λ (nm)	E_g (eV)	m_c/m_0	m_v/m_0	$\lvert\sigma_r\rvert$ (10^{-21} cm^3)		
					Exp.	Theor.[a]	Theor.[b]
ZnSe	532	2.67	0.15[c]	0.78[c]	0.8	1.6	1.6
CdTe	1064	1.44	0.11[d]	0.35[d]	5.0	5.9	5.9
GaAs	1064	1.42	0.07[d]	0.68[d]	6.5	7.2	6.2
ZnTe	1064	2.26	0.12[c]	0.60[c]	0.75	2.4	2.2

[a] BF1, Refs. 27 and 28.
[b] BF2, Refs. 19 and 29.
[c] Effective mass, Ref. 32.
[d] Effective mass, Ref. 33.

which has the same frequency dependence as the enhancement factor in BF1. This agreement is expected, since the same physical mechanism is used in both calculations.

Table 3 lists the calculated values for BF1 and BF2; all three bands are retained in the BF2 calculation (except for ZnTe), compared with the experimental values obtained in this study. In the case of ZnTe the light-hole effective mass was not available, so we used the two-band model. Both models show good agreement with experiment, while the two-band BF1 is simpler.

It is desirable to compare our results with the theory of Banyai and Koch,[34] which includes the effects of electron–hole Coulomb interaction, plasma screening, and band filling. To have a quantitative analysis based on that theory, one needs to have the value for the interband matrix element, which is difficult to calculate from first principles.[35] This value is therefore often determined by comparing the computed and measured linear absorption spectrum. Unfortunately we have not been able to perform this comparison for our thick bulk semiconductor samples. However, when a band-edge absorption coefficient of $\simeq 5 \times 10^4$ cm^{-1} is assumed for all four samples, the values for GaAs and ZnTe agree with experiment, while the value for CdTe is $\simeq 2$ times too small and the value for ZnSe is $\simeq 10$ times too large. Differences in the band-edge absorption among samples could explain this discrepancy.

5. SIMPLE METHOD FOR DETERMINING n_2 AND σ_r

In Ref. 11, in the absence of nonlinear absorption, we showed that the difference in transmittance between the peak and the valley, ΔT_{p-v} in a Z scan, is related to the on-axis phase change at focus, $\Delta\Phi_0$, through the following equation:

$$\Delta T_{p-v} \simeq p^{(i)}\langle\Delta\Phi_0\rangle, \tag{21}$$

where $p^{(3)} \simeq 0.406(1 - S)^{0.25}$ for a third-order nonlinearity and $p^{(5)} \simeq 0.21(1 - S)^{0.25}$ for a fifth-order nonlinearity. S is the linear transmittance through the aperture. When nonlinear absorption is present, dividing the closed-aperture Z-scan data ($S < 1$) by the open-aperture Z-scan data ($S = 1$) gives the approximate contribution from nonlinear refraction. The conditions for the validity of these approximations are detailed in Ref. 11. In addition, Fig. 2, which can be used to determine β directly even at high irradiance levels, shows the contribution of 2PA to the Z-scan signal at focus.

Using relation (21), we empirically find that the following simple procedure gives a quick estimate of γ and σ_r. First a closed-aperture Z scan and an open-aperture Z scan are performed at the same input irradiance, and the closed-aperture data are divided by the open-aperture data. From the resultant curve ΔT_{p-v} is determined, and this value is divided by $p^{(3)}kL_{\text{eff}}I_0/2^{1/2}$. Here α in L_{eff} is taken as $\alpha = \alpha_0 + \beta I_0$. This procedure is performed at various irradiances, and the results of these calculations are plotted as a function of I_0. If there were no higher-order nonlinearities, this procedure would give a horizontal line with vertical intercept γ. Thus, with free-carrier refraction present, the curve is approximately a plot of $\Delta n/I_0$ versus I_0, which is a straight line with an intercept of γ and a slope of $C\sigma_r$, where C is given by

$$C \simeq 0.23(\beta t_0/\hbar\omega) \tag{22}$$

for low linear absorption ($\alpha_0 L < 0.2$). t_0 is the pulse width defined in Eq. (6). In what follows we explain how the coefficient C is obtained. When nonlinear refraction is caused by both a third-order nonlinearity and a fifth-order nonlinearity, we assume that

$$\begin{aligned}\Delta T_{p-v} &\simeq \Delta T_{p-v}^{(3)} + \Delta T_{p-v}^{(5)} \\ &\simeq p^{(3)}\mathbf{k}\langle\Delta n\rangle^{(3)}L_{\text{eff}} + p^{(5)}\mathbf{k}\langle\Delta n^{(5)}\rangle \\ &\quad \times [1 - \exp(-2\alpha L)]/(2\alpha),\end{aligned} \tag{23}$$

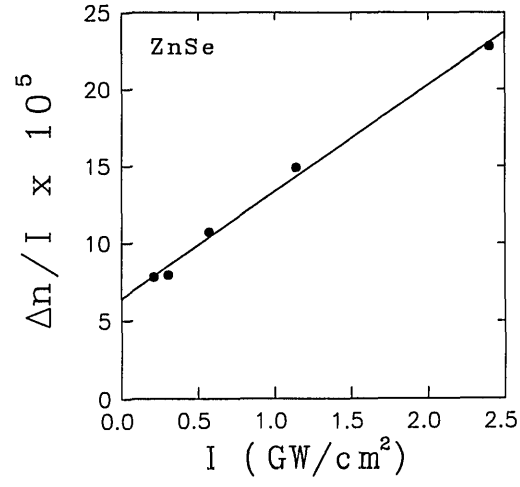

Fig. 10. $\Delta n/I_0$ directly derived from ΔT_{p-v} plotted as a function of I_0 for ZnSe. The intercept of the straight-line best fit to the data yields $\gamma = -6.4 \times 10^{-14}$ cm^2/W, and the slope gives $\sigma_r = -1.1 \times 10^{-21}$ cm^3.

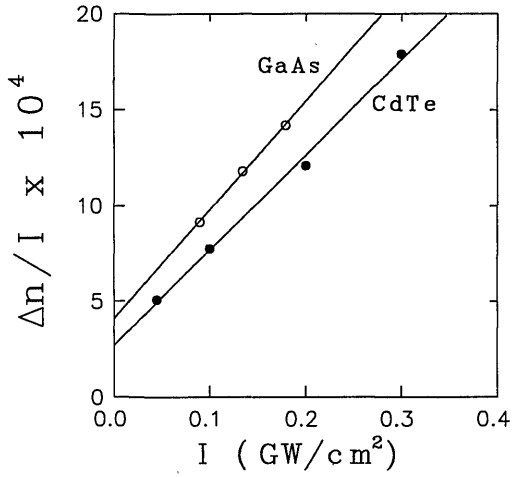

Fig. 11. $\Delta n/I_0$ plotted as a function of I_0 for CdTe (filled circles) and GaAs (open circles). The best fits to the data give $\gamma = -2.7 \times 10^{-13}$ cm^2/W and $\sigma_r = -5.2 \times 10^{-21}$ cm^3 for CdTe and $\gamma = -4.1 \times 10^{-13}$ cm^2/W and $\sigma_r = -5.9 \times 10^{-21}$ cm^3 for GaAs.

$$\langle \Delta n^{(5)} \rangle \simeq \frac{\int_{-\infty}^{\infty} \sigma_r N(t) I_0(t) \mathrm{d}t}{\int_{-\infty}^{\infty} I_0(t) \mathrm{d}t}, \tag{24}$$

where $N(t)$ is given by Eq. (4). Dividing relation (23) by $p^{(3)} k I_0 L_{\mathrm{eff}}/2^{1/2}$, we obtain

$$(\Delta n)/I_0 \simeq \gamma + C\sigma_r I_0, \tag{25}$$

where C is defined by relation (22).

We applied this method to the semiconductors studied in Section 3. For ZnSe at 532 nm we obtain $\gamma = -6.4 \times 10^{-14}$ cm^2/W ($n_2 = -4.1 \times 10^{-11}$ esu) and $\sigma_r = -1.1 \times 10^{-21}$ cm^3. These values were extracted from Fig. 10. In Fig. 11 we show the results of CdTe and GaAs at 1.06 μm. The best fits to the lines gave $\gamma = -2.7 \times 10^{-13}$ cm^2/W ($n_2 = -1.8 \times 10^{-10}$ esu) and $\sigma = -5.9 \times 10^{-21}$ cm^3 for CdTe and $\gamma = -4.1 \times 10^{-13}$ cm^2/W ($n_2 = -3.3 \times 10^{-10}$ esu) and $\sigma = -5.9 \times 10^{-21}$ cm^3 for GaAs. Comparing these values with those obtained in Section 3 by fitting the experimental data, we find that the maximum error is for σ_r of ZnSe and is +37%. In most other cases this procedure gives values within 10% of the previous fits. Therefore the above method is a quick procedure for simultaneously estimating the electronic Kerr effect and the free-carrier refraction in semiconductors.

6. CONCLUSION

We have measured σ_r, the refractive-index change per carrier-pair density, in the presence of two-photon absorption and bound electronic nonlinear refraction in four different semiconductors. This procedure also required us independently to measure both β, the two-photon absorption coefficient, and n_2, the third-order nonlinear refractive index. Thus the applicability of the Z-scan technique has been extended to the measurement of free-carrier refraction. From comparisons of our results with theory, we conclude that σ_r as well as β and n_2 can be predicted within factors of 2 from simple two-band models. The free-carrier refraction is explained well by band-filling models.[19,27–29] β is predicted well by the theory presented in Refs. 24 and 25. n_2 is described well by the theory presented in Refs. 12 and 23, which is based on knowledge of the two-photon absorption spectrum. The agreement between experiment and what can only be described as highly simplified model calculations of complicated band structures of widely differing semiconductors must be attributed to a relative insensitivity of these nonlinear parameters to the details of the band structure. In addition, the effects of higher bands must be minimal. This fortuitous circumstance permits prediction of the nonlinear response with knowledge of only a few basic material constants, namely, the band-gap energy, the linear refractive index, and the photon energy, despite the fact that there are three competing nonlinearities.

ACKNOWLEDGMENTS

We gratefully acknowledge the support of National Science Foundation grant ECS 8617066, the Defense Advanced Research Projects Agency, the Center for Night Vision and Electro-Optics, and the Florida High Technology and Industry Council. In addition, we thank M. Junnarkar and R. DeSalvo for taking portions of the data. We thank A. K. Kar and N. Ross of Heriot-Watt University for providing the ZnSe sample and G. Witt of MIT for the GaAs sample. We also express our appreciation to S. W. Koch and D. C. Hutchings for several informative discussions.

D. J. Hagan is also with the Department of Physics and E. W. Van Stryland with the Departments of Physics and Electrical Engineering, University of Central Florida, Orlando, Florida 32816.

*Present address, Edinburgh Instruments Ltd., Riccarton, Edinburgh EH14 4AP, UK.

REFERENCES AND NOTES

1. D. A. B. Miller, S. D. Smith, and A. M. Johnston, "Optical bistability and signal amplification in a semiconductor crystal: applications of new low power effects in InSb," App. Phys. Lett. **35,** 658 (1979).
2. H. M. Gibbs, S. L. McCall, T. N. Venkatesan, A. C. Gossard, A. Passner, and W. Wiegmann, "Optical bistability in semiconductors," Appl. Phys. Lett. **35,** 451 (1979).
3. A. Miller, and D. Duncan, "Optical nonlinearities in narrow gap semiconductors," in *Optical Properties of Narrow-Gap Low-Dimensional Structures,* C. M. Sotomayor Torres, J. C. Portal, J. C. Maan, and R. A. Stradling, eds. (Plenum, New York, 1987).
4. E. W. Van Stryland, Y. Y. Wu, D. J. Hagan, M. J. Soileau, and K. Mansour, "Optical limiting with semiconductors," J. Opt. Soc. Am. B **5,** 1981 (1988).
5. M. Sheik-Bahae and H. S. Kwok, "Picosecond CO_2 laser-induced self-focusing in InSb," IEEE J. Quantum Electron. **QE-23,** 1974 (1987).
6. S. Guha, E. W. Van Stryland, and M. J. Soileau, "Self-defocusing in CdSe induced by charge carriers created by two-photon absorption," Opt. Lett. **10,** 285 (1985).
7. E. W. Van Stryland, H. Vanherzeele, M. A. Woodall, M. J. Soileau, A. L. Smirl, S. Guha, and T. F. Boggess, "Two photon absorption, nonlinear refraction, and optical limiting in semiconductors," Opt. Eng. **24,** 613 (1985).
8. A. K. Kar, J. G. H. Mathew, S. D. Smith, B. Davis, and W. Prettl, "Optical bistability in InSb at room temperature with two photon absorption," Appl. Phys. Lett. **42,** 334 (1983).

9. E. Canto-Said, D. J. Hagan, J. Young, and E. W. Van Stryland, "Degenerate four-wave mixing measurements of high order nonlinearities in semiconductors," IEEE J. Quantum Electron. **27,** 2274 (1991); D. J. Hagan, E. Canto, E. Meisak, M. J. Soileau, and E. W. Van Stryland, "Picosecond degenerate four-wave mixing studies in ZnSe," in *Conference on Lasers and Electro-Optics,* Vol. 7 of 1988 OSA Technical Digest Series (Optical Society of America, Washington, D.C., 1988), p. 160.
10. A. A. Said, M. Sheik-Bahae, D. J. Hagan, E. J. Canto-Said, Y. Y. Wu, J. Young, T. H. Wei, and E. W. Van Stryland, "Nonlinearities in semiconductors for optical limiting," in *Electro-Optical Materials for Switches, Coatings, Sensor Optics, and Detectors,* R. Hartmann and M. J. Soleau, eds., Proc. Soc. Photo-Opt. Instrum. Eng. **1307,** 294 (1990).
11. M. Sheik-Bahae, A. A. Said, T. H. Wei, D. J. Hagan, and E. W. Van Stryland, "Sensitive measurement of optical nonlinearities using a single beam," IEEE J. Quantum Electron. **26,** 760 (1990).
12. M. Sheik-Bahae, D. J. Hagan, and E. W. Van Stryland, "Dispersion and band-gap scaling of the electronic Kerr effect in solids associated with two-photon absorption," Phys. Rev. Lett. **65,** 96 (1990).
13. M. Sheik-Bahae, A. A. Said, and E. W. Van Stryland, "High-sensitivity, single-beam n_2 measurement," Opt. Lett. **14,** 955 (1989).
14. A. E. Kaplan, "External self-focusing of light by a nonlinear lens," Radiophys. Quantum Electron. **12,** 692 (1969).
15. S. A. Akhmanov, R. V. Khokhlov, and A. P. Sukhorukov, "Self-focusing, self-defocusing, and self-modulation of laser beams," in *Laser Handbook,* F. T. Arecchi and E. O. Shultz-Dubois, eds. (North-Holland, Amsterdam, 1972), Vol. 2, p. 1151.
16. J. H. Bechtel and W. L. Smith, "Two-photon absorption in semiconductors with picosecond pulses," Phys. Rev. B **13,** 3515 (1976).
17. E. W. Van Stryland, M. A. Woodall, H. Vanherzeele, and M. J. Soileau, "Energy band-gap dependence of two-photon absorption," Opt. Lett. **10,** 490 (1985).
18. T. F. Boggess, A. L. Smirl, S. C. Moss, I. W. Boyd, and E. W. Van Stryland, "Optical limiting in GaAs," IEEE J. Quantum Electron. **QE-21,** 488 (1985).
19. D. A. B. Miller, C. T. Seaton, M. E. Prise, and S. D. Smith, "Band-gap-resonant nonlinear refraction in III–V semiconductors," Phys. Rev. Lett. **47,** 197 (1981).
20. J. D. Gaskill, *Linear Systems, Fourier Transforms, and Optics* (Wiley, New York, 1978).
21. The ZnSe sample was obtained from Heriot-Watt University, Edinburgh, UK; CdTe II–VI, from Saxonburgh, Pa.; GaAs from the Massachusetts Institute of Technology, Boston, Mass.; and ZnTe from Cleveland Crystals, Cleveland, Ohio.
22. A. L. Smirl, T. F. Boggess, J. Dubard, and A. G. Cui, "Single and multiple beam nonlinear absorption and refraction measurements in semiconductors," in *Electro-Optical Materials for Switches, Coatings, Sensor Optics, and Detectors,* R. Hartmann and M. J. Soileau, eds., Proc. Soc. Photo-Opt. Instrum. Eng. **1307,** 251 (1990).
23. M. Sheik-Bahae, D. Hutchings, D. J. Hagan, and E. W. Van Stryland, "Dispersion of bound electronic nonlinear refraction in solids," IEEE J. Quantum Electron. **27,** 1296 (1991).
24. M. Weiler, "Nonparabolicity and exciton effects in two photon absorption in zinc-blende semiconductors," Solid State Commun. **39,** 937 (1981).
25. B. S. Wherrett, "Scaling rules for multiphoton interband absorption in semiconductors," J. Opt. Soc. Am. B **1,** 67 (1984).
26. C. C. Lee and H. Y. Fan, "Two photon absorption with exciton effects for degenerate valence bands," Phys. Rev. B **9,** 3502 (1974).
27. A. G. Aronov, D. E. Pikus, and D. Sh. Shekhter, "Quantum theory of free-electron dielectric constant in semiconductors," Sov. Phys. Solid State **10,** 645 (1968).
28. D. H. Auston, S. McAffee, C. V. Shank, E. P. Ippen, and O. Teschke, "Picosecond spectroscopy of semiconductors," Solid State Electron. **21,** 147 (1978).
29. B. S. Wherrett, A. C. Walker, and F. A. P. Tooley, "Nonlinear refraction for cw optical bistability," in *Optical Nonlinearities and Instabilities in Semiconductors,* H. Haug, ed. (Academic, New York, 1988), p. 239.
30. T. S. Moss, "Theory of intensity dependence of refractive index," Phys. Status Solidi B **101,** 555 (1980).
31. E. O. Kane, "Band structure of InSb," J. Chem. Phys. Solids **1,** 249 (1957).
32. K.-H. Hellwege, editor, *Landolt–Börnstein Numerical Data and Functional Relationships in Science and Technology,* Vol. 17, *Semiconductors* (Springer-Verlag, New York, 1982), Subvol. (b).
33. R. K. Jain and M. B. Klein, "Degenerate four-wave mixing in semiconductors," in *Optical Phase Conjugation,* R. A. Fisher, ed. (Academic, New York, 1983), p. 335.
34. L. Banyai and S. W. Koch, "A simple theory for the effects of plasma screening on the optical spectra of highly excited semiconductors," Z. Phys. B **63,** (1986).
35. S. W. Koch, Optical Sciences Center, University of Arizona, Tucson, Ariz. 85721 (personal communication).